Title

Effects of mutation of Asn694 in *Aspergillus niger* α-glucosidase on hydrolysis and transglucosylation

Authors

Min Ma, Masayuki Okuyama*, Megumi Sato, Takayoshi Tagami, Patcharapa Klahan, Yuya Kumagai, Haruhide Mori, and Atsuo Kimura*

Affiliation

Research Faculty of Agriculture, Hokkaido University, Sapporo 060-8589, Japan

* Corresponding authors:

Masayuki Okuyama; Email, okuyama@abs.agr.hokudai.ac.jp; Tel, +81-11-706-2816; Fax, +81-11-706-2808

Atsuo Kimura; Email, kimura@abs.agr.hokudai.ac.jp; Tel and Fax, +81-11-706-2808

Abstract

Aspergillus niger α-glucosidase (ANG), a member of glycoside hydrolase family 31, catalyzes hydrolysis of α-glucosidic linkages at the non-reducing end. In the presence of high concentrations of maltose, the enzyme also catalyzes the formation of α-(1→6)-glucosyl products by transglucosylation and it is used for production of the industrially useful panose and isomaltooligosaccharides. The initial transglucosylation by wild-type ANG in the presence of 100 mM maltose [Glc(α1-4)Glc] yields both α-(1→6)- and α-(1→4)-glucosidic linkages, the latter constituting ~25% of the total transfer reaction product. The maltotriose [Glc(α1-4)Glc(α1-4)Glc], α-(1→4)-glucosyl product disappears quickly, whereas the α-(1→6)-glucosyl products panose [Glc(α1-6)Glc(α1-4)Glc], isomaltose [Glc(α1-6)Glc], and isomaltotriose [Glc(α1-6)Glc(α1-6)Glc] accumulate. To modify the transglucosylation properties of ANG, residue Asn694, which was predicted to be involved in formation of the plus subsites of ANG, was replaced with Ala, Leu, Phe, and Trp. Except for N694A, the mutations enhanced the initial velocity of the α-(1→4)-transfer reaction to produce maltotriose, which was then degraded at a rate similar to that by wild-type ANG. With increasing reaction time, N694F and N694W mutations led to the accumulation of larger amounts of isomaltose and isomaltotriose than achieved with the wild-type enzyme. In the final stage of the reaction, the major product was panose (N694A and N694L) or isomaltose (N694F and N694W).

Keywords

α-glucosidase, transglucosylation, isomaltooligosaccharides, *Aspergillus niger*, structural element, site-directed mutagenesis

Introduction

Prebiotics are oligosaccharides used selectively by beneficial bacteria, including the genera *Bifidobacterium* and *Lactobacillus*, and regular dietary intake of prebiotics has been shown to improve human health. The conversion of these compounds to short-chain fatty acids such as acetate, propionate, and butyrate improves food intake, reduces inflammatory activity, and promotes insulin signaling (Hur and Lee 2015). The main groups of prebiotics are fructooligosaccharides and galactooligosaccharides. Other beneficial prebiotic carbohydrates include isomaltooligosaccharides (IMOs), xylooligosaccharides, soybean oligosaccharides, lactosucrose, and mannooligosaccharides (Kothari et al. 2014).

Among the prebiotic effects of IMOs, panose (PN; α-D-glucopyranosyl-(1→6)-α-D-glucopyranosyl-(1→4)-D-glucopyranose), and other oligosaccharides containing α-(1→6)-glucosidic linkage(s) is an increase in the number of bifidobacteria in the intestinal flora (Kohmoto et al. 1988, 1991), especially in response to the disaccharide and trisaccharide fractions of IMO (Kaneko et al. 1994). PN also promotes significant growth of bifidobacteria in both test cultures and simulations of colonic fermentation (Mäkeläinen et al. 2009; Kohmoto et al. 1992). The industrial production of α-(1→6)-glucosidic bond-containing saccharides was achieved by the α-glucosidase-catalyzed transglucosylation of maltose (G2) (Takaku 1988), in a reaction using the α-glucosidase from *Aspergillus niger* (ANG), which belongs to glycoside hydrolase family 31 (GH31). The ability of ANG to catalyze the formation α-(1→6)-glucosidic linkages has led to substantial interest in this enzyme.

α-Glucosidase hydrolyzes the α-glucosidic linkage at the nonreducing end of the substrate. In the presence of high substrate concentrations, the enzyme also catalyzes transglucosylation, which transfers a glucosyl moiety from the donor substrate to the OH-group of the acceptor substrate. The double-displacement mechanism employed by the enzyme progresses through a glycosyl-enzyme intermediate, which involves two functional groups: a catalytic nucleophile and a general acid/base catalyst. The latter transfers a proton to the glucosidic linkage, followed by departure of a leaving group from the substrate. Simultaneously, the nucleophile attacks the anomeric carbon to form the

intermediate. Hydrolysis results from decomposition (deglycosylation) of the intermediate in a reaction involving a water molecule, with activation assisted by the general base catalyst. Transglucosylation progresses through the same deglycosylation step but with the OH-group from the sugar (alcohol) molecule replacing the water molecule. At high concentrations of G2, α-glucosidase initially synthesizes PN (Fig. 1A) and maltotriose (G3) (Fig. 1B) with α-(1→6) and α-(1→4) transfers, respectively. With increasing amounts of glucose derived from concomitant hydrolysis and released during the glycosylation step, the enzyme generates isomaltose (IG2) (Fig. 1C), and IG2 can act as a further acceptor species for isomaltotriose (IG3) production (Fig. 1D). Transfer to the 2-OH or 3-OH moiety [with the respective formation of kojibiose (KJ) or nigerose (NR)] occurs occasionally. The mechanism of this reaction suggests that the structural element needed for transglucosylation is present at subsite +1 and/or +2 (Fig. 1). Since no three-dimensional structure of ANG is available, we predicted Asn694 to be a candidate residue at the plus subsites based on the structures of homologous GH31 proteins.

In this study, we constructed four mutant enzymes, N694A/L/F/W, the hydrolytic activity of which suggested the contribution of Asn694 to the plus subsites. We analyzed the transglucosylation products generated from high concentrations of G2 in its reaction with wild-type ANG and the four Asn694 variants. The results showed that in the initial stage of the reaction, the wild-type enzyme catalyzed the formation of both α-(1→4)- and α-(1→6)-glucosidic linkages. N694L/F/W altered the specificity of the transglucosylation, implicating Asn694 as a structural element that regulates the transglucosylation products of ANG.

Materials and methods

Production of Asn694-mutated ANGs

Site-directed mutagenesis of Asn694 was performed according to the manual of the PrimeSTAR mutagenesis basal kit (Takara Bio, Shiga, Japan) using a template [an expression vector (Tagami et al. 2013a) harboring mature ANG cDNA] and primers (Table 1). The nucleotide sequences of the resultant products were analyzed using an ABI PRISM 310 genetic analyzer (Thermo-Applied

Biosystems, Carlsbad, CA, USA). The production and purification of mutant ANGs were performed as previously described (Tagami et al. 2013a). The purity of the enzymes was determined by SDS-PAGE. The concentration of the isolated protein was estimated by amino acid analysis of the protein hydrolysate (6 M HCl, 110°C, 24 h) using a JLC-500/V system (Nihon Denshi, Tokyo, Japan) followed by analysis using a ninhydrin-detection system.

Enzyme activity was measured at 37°C for 9 min using a standard reaction mixture consisting of 0.2% (w/v) G2 (Nihon Shokuhin Kako, Tokyo, Japan), 40 mM sodium acetate buffer (pH 4.0), 0.02% Triton X-100, and the appropriate concentration of enzyme. The reaction was terminated by the addition of 100 μL 2 M Tris-HCl (pH 7.0). Liberated glucose was quantified using the glucose C-II test (Wako Pure Chemical Industry, Osaka, Japan). One unit of activity was defined as the amount of enzyme hydrolyzing 1 μmol of G2 per min in the above conditions.

Influence of pH and temperature on activity

The optimum pH for activity of the Asn694 mutants was evaluated in the standard reaction conditions, except that Britton-Robinson buffer (40 mM acetic acid, 40 mM phosphoric acid and 40 mM boric acid; pH adjusted with NaOH; pH 2.3–8.3) was substituted for acetate buffer. The enzymes were used at the following concentrations: 0.80 nM for N694A, 0.51 nM for N694L, 0.64 nM for N694F, and 0.40 nM for N694W.

To investigate pH stability, N694A (79 nM), N694L (51 nM), N694F (64 nM), or N694W (40 nM) was incubated at 4°C for 24 h in 10-fold-diluted Britton-Robinson buffer (pH 3.0–11.5) containing 0.1% Triton X-100. The activities of N694L and N694W at pH 2.3–3.2 were evaluated using McIlvaine buffer (0.2 M $NaHPO_4$, with the pH adjusted by the addition of 0.1 M citric acid). Residual activity was measured in standard assay conditions. The stable region was defined as the pH range exhibiting residual activity >90% of the original activity.

The thermostability of N694A (4.0 nM), N694L (2.6 nM), N694F (3.2 nM), and N694W (2.0 nM) was determined by respectively incubating the enzyme in 20 mM sodium acetate buffer (pH 4.0) containing 0.1% Triton X-100 at 37–70°C for 15 min, after which the residual activity was measured

123 in standard assay conditions. The stable region was determined as described above.

124

125 **Characterization of hydrolysis and transglucosylation**

126 The substrates used to measure the hydrolysis rate were G2, G3, maltotetraose (G4), maltopentaose
127 (G5), maltohexaose (G6), maltoheptaose (G7), KJ, NR (Wako Pure Chemical Industry), IG2, and PN
128 (Tokyo Chemical Industry, Tokyo, Japan). The kinetic parameters k_{cat} and K_m were calculated in
129 KaleidaGraph 3.6J (Synergy Software, Reading, PA, USA) from a weighted fit of the Michaelis-
130 Menten equation to the initial velocities at eight substrate concentrations, ranging from one-third- to
131 three-fold the K_m value. The experiments were repeated three times and mean and standard deviation
132 values were calculated. k_{cat}/K_m values were calculated from the mean values of k_{cat} and K_m. The
133 concentrations of enzyme were: wild-type ANG (1.3–2.9 nM), N694A (0.35–4.0 nM), N694L (0.73–
134 5.1 nM), N694F (0.43–3.2 nM), and N694W (0.27–8.1 nM).

135 The initial transglucosylation velocity (v_{tg}) of wild-type or mutated ANG was analyzed using G2
136 as the substrate. A reaction mixture consisting of 100 mM G2, enzyme (wild-type, 4.2 nM; N694A,
137 3.2 nM; N694L, 1.7 nM; N694F, 2.6 nM; N694W, 2.0 nM), and 40 mM sodium acetate buffer (pH
138 4.0) was incubated at 37°C. After 2, 4, 8, 12, and 15 min, the reaction was terminated by heating at
139 100°C for 3 min. The concentrations of glucose, G2, G3, PN, and centose [CT; 2,4-di-*O*-(α-glucosyl)-
140 glucose] were measured by high-performance anion-exchange chromatography with pulsed
141 amperometric detection (HPAEC-PAD; Dionex ICS-3000 system; Dionex/Thermo Fisher Scientific,
142 Idstein, Germany) using a CarboPac PA1 column (4 × 250 mm; Dionex/Thermo Fisher Scientific).
143 Carbohydrates were separated by isocratic elution with 400 mM NaOH at a flow rate of 0.8 mL min^{-1}.
144 Standard CT was prepared as described by Song et al. (2013). The v_{tg} was defined as the sum of the
145 initial generation rates of PN, G3, and CT (v_{PN}, v_{G3}, and v_{CT}, respectively) on the supposition that
146 only G2 was used as an acceptor molecule in the initial reaction. The hydrolysis velocity (v_h) was
147 calculated from both v_{tg} and the glucose-production rate (v_{glc}): $v_h = (v_{glc} - v_{tg})/2$. The percentage
148 of transglucosylation in the total reaction (R_{tg}) was estimated as: $R_{tg} = v_{tg}/(v_h + v_{tg}) \times 100 = 2 \times v_{tg}$
149 $/(v_{glc} + v_{tg}) \times 100$. The proportion of α-(1→4) ($R_{(1,4)}$) or α-(1→6) ($R_{(1,6)}$) transfer reactions vs. the

total transglucosylation was calculated from the equations: $R_{(1,4)} = v_{G3} /(v_{PN} + v_{G3} + v_{CT}) \times 100$ and $R_{(1,6)} = v_{PN}/(v_{PN} + v_{G3} + v_{CT}) \times 100$.

The time courses of the formation of the transglucosylation products were analyzed using reaction mixtures consisting of 100 mM G2 and 1.0 U/mL of each enzyme in 40 mM sodium acetate buffer (pH 4.0). The reactions were incubated at 37°C and samples were taken at 0, 0.5, 1.0, 1.5, 2.0, 2.5, and 3.0 h. A 3-min incubation at 100°C terminated the reactions. The concentration of each product was determined by HPAEC-PAD analysis, as described above.

Results

Selection of target residue for mutagenesis

As Fig. 1 shows, the transglucosylation of ANG occurs when G2 molecule binds to the +1/+2 subsites as an acceptor substrate. Modification of these subsites would thus affect the transglucosylation features of the enzyme. As no three-dimensional structure of ANG is available, we predicted the subsite structure from ligand-complexed homologous proteins of GH31. Sugar beet α-glucosidase (SBG) (Tagami et al. 2013b), the N-terminal subunit of maltase-glucoamylase (NtMGAM) (Sim et al. 2008), and its C-terminal subunit (CtMGAM) (Ren et al. 2011) were the highest ranked homologs for ANG among the GH31 enzymes of known structure based on HHpred (Söding et al. 2005). Using the Bioinformatics Toolkit server (http://toolkit.tuebingen.mpg.de/), we built a model structure of ANG using the structure of SBG, which displayed the best probability, E-value, and score with ANG in HHpred. The model structure showed that the +1/+2 subsites of ANG were formed by Asp225, Thr228, Trp343, Trp453, Phe497, Arg644, Phe693, and Asn694 (Fig. 2A). All residues except Thr228, Trp343 and Asn694 were conserved among GH31 α-glucosidases, and thus these residues are probably required for the generic properties of GH31 α-glucosidases. We previously demonstrated that replacement of Thr228 with Phe resulted in creation of a +3 subsite in ANG (Tagami et al. 2013a). An aromatic residue equivalent to Trp343 was proved to be involved in selectivity of α-(1→4) and α-(1→6) glucosidic linkages in both hydrolysis and transglucosylation by homologous enzymes (Tan et al. 2010; Ren et al. 2011; Song et al. 2013). However, mutational analysis of a residue equivalent

177 to Asn694 has not been performed and its role in the catalytic reaction remains obscure. Asn694 is
178 on β→α loop 7 of a catalytic TIM barrel domain and is positioned near the +2 subsite in the model
179 structure. The relevant residue varies among GH31 α-glucosidases (Fig. 2B). In CtMGAM, Phe1560,
180 corresponding to Asn694, is involved in the formation of +1/+2/+3 subsites (Fig. 2A).
181 *Schwanniomyces occidentalis* α-glucosidase (SOG), which is similar to ANG in both hydrolysis and
182 transglucosylation specificities (Song et al. 2013), also has Asn674 at the corresponding position. We
183 therefore hypothesized that Asn694 is involved in the specificities of the hydrolytic reaction and
184 transglucosidation, and its mutation might affect their specificities. Hydrophobic residues of various
185 size, Ala, Leu, Phe, and Trp, were selected as alternate residues for Asn, to increase the hydrophobic
186 interactions between the enzyme and substrate, and to change the specificities.
187
188 **Production of Asn694-mutated ANGs**
189 The mutant ANGs (N694A/L/F/W) were produced in *Pichia pastoris* and purified by Ni-affinity
190 chromatography (Tagami et al. 2013a). On SDS-PAGE, each isolated mutant enzyme displayed the
191 same broad, single band as obtained with the wild-type enzyme (Fig. S1). The specific activities of
192 the mutants were: 152 U/mg (N694A), 120 U/mg (N694L), 185 U/mg (N694F), and 155 U/mg
193 (N694W). The stable pH ranges and the optimum pH for G2 hydrolysis were almost the same in the
194 mutants and the wild-type, except for the optimum pHs of N694L and N694F (4.8 and 4.7,
195 respectively), which were slightly higher than that of the wild-type (pH 4.0) (Tagami et al. 2013a)
196 (Fig. S2). The thermal stability was slightly reduced in N694L, for which the residual activity after
197 treatment at 60°C for 15 min was 70%, but the other forms of the enzyme exhibited >80% residual
198 activity after treatment in the same conditions.
199
200 **Kinetic analysis of hydrolysis activities of Asn694 mutants**
201 Table 2 summarizes the kinetic parameters of the Asn694-mutated ANGs for a series of
202 maltooligosaccharides, α-glucobioses, and PN. The k_{cat} values of N694A were 65–95% of those of
203 the wild-type enzyme, among which the values for NR and IG2 were explicitly decreased. The K_m

values of N694A were similar to those of the wild-type enzyme, but increased slightly for α-glucobioses. Of the four mutated ANGs, N694L had the lowest k_{cat}/K_m values. Its k_{cat} values for trisaccharides (G3 and PN) were nearly the same as those of wild-type ANG, while for other substrates the k_{cat} values of the mutant were 33–84% of the wild-type values. The K_m values of N694L were 1.3–3.5-fold higher than those of the wild-type enzyme. The higher K_m values for G3 and PN decreased the k_{cat}/K_m values by 35% and 30% compared with the wild-type, respectively. The k_{cat}/K_m values for other substrates of N694L were also decreased to 14−48% of the wild-type level. In contrast, the k_{cat} values of N694F were 1.1–1.7 times higher than those of the wild-type enzyme for substrates other than KJ, IG2, and PN. This mutation was associated with a 1.1–2.5-fold increase in the K_m values for all substrates except IG2. The k_{cat}/K_m values of N694F were in the range of 75%–110% of that of the wild-type enzyme, with a significant decrease observed for G2 (51%), IG2 (64%), and PN (27%). The k_{cat} values of N694W were 29–90% of those of the wild-type, but for G2 the value was higher. The K_m values of this mutant generally decreased relative to the wild-type, with the exceptions of increases for the substrates G2, KJ, NR, and PN.

Transglucosylation by wild-type and mutant ANGs

The transglucosylation properties of wild-type ANG were investigated because little is known about its initial behavior at high substrate concentrations. The reaction products synthesized from 100 mM G2 in 15 min were glucose, PN, G3, and CT, with v_{glc}, v_{PN}, v_{G3}, and v_{CT} values of 980, 314, 101, and 24.3 s^{-1} M^{-1}, respectively (Fig. S3, Table 3). R_{tg} was 62%, and $R_{(1,4)}$ and $R_{(1,6)}$ were 23% and 72%, respectively. Thus, wild-type ANG possessed notable α-(1→4)-linkage formation ability. In further reaction with G2, the main transglucosylation products were PN and G3 during the first hour, after which G3 disappeared and IG2 accumulated (Fig. 3A). The concentration of PN increased until 2 h, followed by a gradual decrease. At the end of the reaction (3 h), IG2 and PN were the major transglucosylation products, with traces of IG3, KJ, and CT (Fig. 3A3).

Transglucosylation by the Asn694 variants was also examined (Table 3). The initial transglucosylation velocities of N694A and N694F were the same as those of wild-type ANG except

231 for v_{G3} of N694F. Neither N694L nor N694W could detectably synthesize CT (detection limit 8×10^{-3}
232 mM). All mutant ANGs except N694A had an increased v_{G3} compared with wild-type ANG. The 2.0-,
233 3.7-, and 1.9-fold greater velocities for N694L, N694F, and N694W, respectively, resulted in 37, 53,
234 and 41% higher $R_{(1,4)}$ values, respectively. N694A exhibited similar $R_{(1,4)}$ and $R_{(1,6)}$ to the wild-type
235 enzyme. R_{tg} was nearly the same for N694L and the wild-type (58%), but for the mutant, the $R_{(1,6)}$
236 value decreased to 63%. Transglucosylation by N694F was considerably altered: R_{tg} increased
237 slightly compared with wild-type ANG, but $R_{(1,6)}$ decreased to 43%. The R_{tg} of N694W was also
238 slightly increased, while $R_{(1,6)}$ was 59%.

239 Figure 3B–E depict the time courses of the transglucosylation products formed by the mutant
240 enzymes during the 3-h reaction; in all cases, >90% of the G2 had been consumed at 2 h (Fig. 3B2–
241 E2). The reaction profiles of N694A and N694L were similar to that of wild-type ANG (Fig. 3B and
242 C), with early production of PN and G3 and an increase in IG2, as well as a gradual decrease in PN
243 towards the end. One difference was the production of IG2, the amounts of which at 3 h were slightly
244 lower in the N694A and N694L reactions than in the wild-type reaction. Another difference was an
245 earlier decrease in G3 than in the wild-type reaction profile (beginning at 0.5 h for the mutants but
246 at 1 h for the wild-type enzyme) (Fig 3A3–E3). This earlier decrease of G3 was also observed in
247 N694F and N694W reactions. N694F and N694W exhibited reaction profiles distinct from that of the
248 wild-type (Fig. 3D1 and E1). At the beginning of the reaction (30 min), these two mutants produced
249 larger amounts of IG2 and G3, followed by rapid (N694F) or abundant (N694W) accumulation of
250 IG2. While PN formation at 30 min was almost identical for these two mutants and the wild-type
251 enzyme, after reaching its maximum level, the PN concentration either remained within a constant
252 range (N694F) or declined very modestly (N694W). IG3 synthesis by N694F and N694W was also
253 higher than that by the wild-type enzyme. Figure 4 shows the composition of the transglucosylation
254 products at 3 h, the end of the recorded reaction. IG2 and PN were the predominant final products of
255 wild-type ANG in almost identical amounts, whereas PN predominated over IG2 in the reactions
256 catalyzed by N694A and N694L, with the latter enzyme having the highest percentage of PN
257 accumulation among the mutant ANGs. N694F and N694W yielded larger percentages of IG2 and

IG3 than were obtained with the other enzymes, with N694W resulting in the greatest accumulation of IG2.

Discussion

To investigate the role of Asn694 in hydrolytic activity and the transglucosylation reaction of ANG, we constructed N694A/L/F/W variants. We first investigated their hydrolytic activity. The results of the kinetic analysis of N694A suggested the involvement of Asn694 in the +1 subsite. The k_{cat}/K_m value of N694A for G2 was 70% of that for the wild-type enzyme, while there was only a slight decrease in the corresponding values for the other maltooligosaccharides. The mutation of Asn694 to Ala, of which the side chain was non-bulky and chemically inert, might have lowered the affinity at the +1 subsite and thus affected the k_{cat}/K_m value for G2. Meanwhile, the affinity at the +2 subsite can offset the lowering of +1 subsite affinity, and thus the effect on the k_{cat}/K_m values for the other maltooligosaccharides was small. However, the position of Asn694 seems to be close to +2 subsite in the model structure. Indeed, N694F displayed a slightly higher k_{cat}/K_m for G3 compared with wild-type ANG, indicating that substitution of Asn with Phe moderately enhanced the affinity at the +2 subsite. CtMGAM has Phe1560 at the relevant position, and its aromatic side chain is encircled by three sugar rings of acarbose (Fig. 2A), allowing it to closely associate with the formation of the +1 and +2 subsites (Ren et al. 2011). It is possible that maltooligosaccharide substrates bind to N694F in a similar manner to CtMGAM and thus the mutation in ANG causes slight enhancement of the affinity at the +2 subsite. A lower k_{cat}/K_m for G2 and its recovery for G3 were observed in N694A as well as N694F and N694W. This kinetic behavior might be explained by the size of the side chains. The change in size of the residue 694 side chain on mutation could affect the orientation of Phe693, which is conserved in GH31 α-glucosidases and closer to the +1 subsite than Asn694 (Fig. 2A). This change in orientation might cause impairment of the +1 subsite and thus the decrease in k_{cat}/K_m for G2. In N694L, this kinetic behavior was not observed, which could be rationalized as being due to the similar size of the side chains of Leu and Asn. Among the mutant enzymes, the lowest k_{cat}/K_m values for all substrates tested were those of N694L. The N694L mutation could negatively affect the

285 function of the general acid/base catalyst. In the modeled structure, Asn694 is located relatively close
286 to Asp660, which serves as the general acid/base catalyst (Fig. 2A). Indeed, a shift in the optimum
287 pH of the hydrolytic activity was observed in N694L. It is possible that increasing the hydrophobicity
288 by this mutation disturbs the ionic state of the general acid/base catalyst. Meanwhile, the optimum
289 pH for N694F also shifted, but its kinetic parameters exhibited no significant decrease compared with
290 the wild-type. The mechanism underlying the decrease in the activity of N694L is unclear.

291 Taken together, Asn694 is likely involved in substrate binding at subsite +2. Our previous report
292 mentioned the involvement of Thr228 on the N-loop of ANG in the formation of the plus subsites
293 (Tagami et al.2013a). Thr228 and Asn694 are located on the N-loop and the β→α loop 7, respectively,
294 but these might be spatially close together based on the model structure (Fig. 2A). It is likely that the
295 plus subsites of ANG are formed by the N-loop and the β→α loop 7.

296 Next, transglucosylation by wild-type ANG and its Asn694 variants were investigated. Formation
297 of the α-(1→6)-glucosidic linkage during wild-type ANG-catalyzed transglucosylation is well-
298 established. The NMR study by Shimba et al. (2009) indicated that prolonged reaction of the enzyme
299 resulted in the efficient production of an α-(1→6)-glucosidic linkage. However, analysis of the initial
300 transglucosylation revealed that the wild-type enzyme catalyzed not only α-(1→6) but also α-(1→4)
301 transfer, with the latter accounting for 25% of the total transglucosylation (Table 3). G3, produced
302 together with PN, decreased quickly, as expected from the very high k_{cat}/K_m value for this substrate
303 (Table 2). In the double displacement catalytic mechanism, the k_{cat}/K_m for hydrolysis is an apparent
304 second-order rate constant that refers to the properties and the reactions of a free enzyme and free
305 substrate (Fersht 1988). Therefore, the G3 produced may be preferentially bound to the enzyme and
306 may either be hydrolyzed or used as the donor substrate for transglucosylation. As the concentration
307 of glucose increased as a product of hydrolysis and transglucosylation (glucose from the reducing-
308 end of donor G2), free glucose became an acceptor substrate for IG2 formation (Fig. 3A1 and A2).
309 The k_{cat}/K_m value for PN hydrolysis was higher than that for IG2, such that PN was gradually
310 degraded and IG2 accumulated. IG2 then became the acceptor in the transglucosylation reaction,
311 which yielded IG3 in the late stages of the reaction (Fig. 3A3).

312 The v_{G3} values of the mutants N694L, N694F, and N694W were significantly higher than that of
313 wild-type ANG (Table 3), but their v_{PN} values were comparable. This phenomenon was especially
314 pronounced in N694F, in which v_{G3} exceeded v_{PN} and $R_{(1,4)}$ was 53%. The higher relative k_{cat}/K_m
315 values for G3 and PN $[(k_{cat}/K_m)_{G3}/(k_{cat}/K_m)_{PN}]$ seem to be related to the higher $R_{(1,4)}$.
316 $(k_{cat}/K_m)_{G3}/(k_{cat}/K_m)_{PN}$ for N694F was 28.1, greater than that for the wild-type (7.1). However,
317 higher $(k_{cat}/K_m)_{G3}$ also means G3 is more likely to act as a substrate for hydrolysis or as the donor
318 for the next transglucosylation. As a result, the concentration of G3 decreased steeply and most of
319 the G3 formed was then consumed in the late stages of the reaction (Fig. 3C–E).
320 Larger amounts IG2 and IG3 were accumulated by N694F and N694W than by the wild-type, a
321 finding attributable to increased nonproductive binding of IG2. Kinetic analysis of the mutants
322 showed that the mutations decreased both k_{cat} and K_m, but had little effect on k_{cat}/K_m for IG2 (Table
323 2). This behavior is typical for the nonproductive binding of substrate. The increased nonproductive
324 binding of IG2, which probably occupies the +1 and +2 subsites, would facilitate the accumulation
325 of IG2, by decreasing the rate of its hydrolysis and thus enhancing its function as an acceptor
326 molecule, resulting in the generation of IG3 (Fig. 1C).
327 This study revealed that ANG inherently transfers α-(1→4)-glucosidic linkages, accounting for
328 ~25% of the total transfer reactions catalyzed by the enzyme. The mutation of Asn694 to Phe or Trp
329 enhanced the α-(1→4)-glucosyl transfer activity and thus the efficient production of G3 from G2
330 during the initial reaction; thereafter, there was no accumulation of G3 because of its very high
331 k_{cat}/K_m value. Two mutants, N694F and N694W, accumulated significantly more of the industry-
332 useful IG2 and IG3 in the prolonged reaction, probably owing to the increase in nonproductive
333 binding resulting from the mutations. Thus, mutation is an extremely valuable approach to achieve
334 glycoside-hydrolase-associated oligosaccharide synthesis. Although regulation of the glycoside-
335 hydrolase-catalyzed synthesis of glycosidic linkages by mutation is challenging, using the mutants
336 obtained in this study we were able to improve the transglucosylation specificity of ANG. One of the
337 significant results of this study is that mutant enzymes exhibiting commercially interesting
338 transglucosylation properties can be generated without reducing the activity, as often occurs

following the engineering of residues within/near the active site.

Acknowledgments

We thank the staff of the Instrumental Analysis Division of the Creative Research Institution at Hokkaido University for amino acid analysis. This study was supported in part by the JSPS KAKENHI Grant Number JP26292049 (Atsuo Kimura), and by the JSPS and NRF under the Japan-Korea Basic Science Cooperation Program (Atsuo Kimura).

Conflict of interest

The authors declare that they have no competing interests.

Compliance with Ethical Standards

This article does not describe any studies on human participants or animals performed by any of the authors.

References

Fersht A (1988) Structure and mechanism in protein science: a guide to enzyme catalysis and protein folding. W H Freeman and Company, New York

Hur KY, Lee M-S (2015) Gut microbiota and metabolic disorders. Diabetes Metab J 39:198–203. doi:10.4093/dmj.2015.39.3.198

Kaneko T, Kohmoto T, Kikuchi H, Shiota M, Iino H, Mitsuoka T (1994) Effects of isomaltooligosaccharides with different degrees of polymerization on human fecal bifidobactcria. Biosci Biotechnol Biochem 58:2288–2290. doi:10.1271/bbb.58.2288

Kohmoto T, Fukui F, Takaku H, Machida Y, Arai M, Mitsuoka T (1988) Effect of isomalto-oligosaccharides on human fecal flora. Bifidobact Microflora 7:61–69. doi:10.12938/bifidus1982.7.2_61

Kohmoto T, Fukui F, Takaku H, Mitsuoka T (1991) Dose-response test of isomaltooligosaccharides

366 for increasing fecal bifidobacteria. Agric Biol Chem 55:2157–2159.
367 doi:10.1080/00021369.1991.10870921
368 Kohmoto T, Tsuji K, Kaneko T, Shiota M, Fukui F, Takaku H, Nakagawa Y, Ichikawa T, Kobayash
369 S (1992) Metabolism of ^{13}C-isomaltooligosaccharides in healthy men. Biosci Biotechnol
370 Biochem 56:937–940. doi:10.1271/bbb.56.937
371 Kothari D, Patel S (2014) Therapeutic spectrum of nondigestible oligosaccharides: overview of
372 current state and prospect. J Food Sci 79:R1491–R1498. doi:10.1111/1750-3841.12536
373 Mäkeläinen H, Hasselwander O, Rautonen N, Ouwehand AC (2009) Panose, a new prebiotic
374 candidate. Lett Appl Microbiol 49:666–672. doi:10.1111/j.1472-765X.2009.02698.x
375 Ren L, Qin X, Cao X, Wang L, Bai F, Bai G, Shen Y (2011) Structural insight into substrate
376 specificity of human intestinal maltase-glucoamylase. Protein Cell 2:827–836.
377 doi:10.1007/s13238-011-1105-3
378 Shimba N, Shinagawa M, Hoshino W, Yamaguchi H, Yamada N, Suzuki E (2009) Monitoring the
379 hydrolysis and transglycosylation activity of α-glucosidase from *Aspergillus niger* by nuclear
380 magnetic resonance spectroscopy and mass spectrometry. Anal Biochem 393:23–28.
381 doi:10.1016/j.ab.2009.06.002
382 Sim L, Quezada-Calvillo R, Sterchi EE, Nichols BL, Rose DR (2008) Human intestinal maltase–
383 glucoamylase: crystal structure of the N-terminal catalytic subunit and basis of inhibition and
384 substrate specificity. J Mol Biol 375:782–792. doi:10.1016/j.jmb.2007.10.069
385 Söding J, Biegert A, Lupas AN (2005) The HHpred interactive server for protein homology detection
386 and structure prediction. Nucleic Acids Res 33:W244–W248. doi:10.1093/nar/gki408
387 Song KM, Okuyama M, Nishimura M, Tagami T, Mori H, Kimura A (2013) Aromatic residue on β
388 →α loop 1 in the catalytic domain is important to the transglycosylation specificity of
389 glycoside hydrolase family 31 α-glucosidase. Biosci Biotechnol Biochem 77:1759–1765.
390 doi:10.1271/bbb.130325
391 Takaku H (1988) Anomalously linked oligosaccharides mixture. In: The amylase research society of
392 Japan (ed) Handbook of amylases and related enzymes. Pergamon press, Oxford, pp 215-217

393 Tagami T, Okuyama M, Nakai H, Kim YM, Mori H, Taguchi K, Svensson B, Kimura A (2013a) Key
394 aromatic residues at subsites + 2 and + 3 of glycoside hydrolase family 31 α-glucosidase
395 contribute to recognition of long-chain substrates. Biochim Biophys Acta - Proteins
396 Proteomics 1834:329–335. doi:10.1016/j.bbapap.2012.08.007
397 Tagami T, Yamashita K, Okuyama M, Mori H, Yao M, Kimura A (2013b) Molecular basis for the
398 recognition of long-chain substrates by plant α-glucosidases. J Biol Chem 288: 19296–19303.
399 doi:10.1074/jbc.M113.465211
400 Tagami T, Yamashita K, Okuyama M, Mori H, Yao M, Kimura A (2015) Structural advantage of
401 sugar beet α-glucosidase to stabilize the Michaelis complex with long-chain substrate. J Biol
402 Chem 290:1796–1803. doi:10.1074/jbc.M114.606939
403 Tan K, Tesar C, Wilton R, Keigher L, Babnigg G, Joachimiak A (2010) Novel α-glucosidase from
404 human gut microbiome: substrate specificities and their switch. FASEB J 24:3939–3949. doi:
405 10.1096/fj.10-156257
406

407 **Table 1** Sequences of oligonucleotides used for PCR in this study

	Direction	Sequence (5′→3′)
N694A_s	sense	GGGTTTGCTGGAAACTCCGATGAGGAG
N694A_a	antisense	GTTTCCAGCAAACCCACAGGTGTCCGC
N694L_s	sense	GGGTTTTTAGGAAACTCCGATGAGGAG
N694L_a	antisense	GTTTCCTAAAAACCCACAGGTGTCCGC
N694F_s	sense	GGGTTTTTTGGAAACTCCGATGAGGAG
N694F_a	antisense	GTTTCCAAAAAACCCACAGGTGTCCGC
N694W_s	sense	GGGTTTTGGGGAAACTCCGATGAGGAG
N694W_a	antisense	GTTTCCCCAAAACCCACAGGTGTCCGC

408 Mutated codons are underlined.

Table 2 Kinetic parameters of wild-type and mutated ANGs

	Wild type [a]			N694A			N694L		
Substrate [b]	k_{cat}	K_m	k_{cat}/K_m	k_{cat}	K_m	k_{cat}/K_m	k_{cat}	K_m	k_{cat}/K_m
	s^{-1}	mM	s^{-1} mM^{-1}	s^{-1}	mM	s^{-1} mM^{-1}	s^{-1}	mM	s^{-1} mM^{-1}
G2	509 ± 5	0.913 ± 0.010	558	466 ± 7	1.18 ± 0.06	395	388 ± 2	3.23 ± 0.07	120
G3	475 ± 11	0.609 ± 0.025	779	450 ± 4	0.634 ± 0.012	709	497 ± 5	1.82 ± 0.05	274
G4	416 ± 10	0.823 ± 0.032	505	361 ± 3	0.775 ± 0.028	465	351 ± 6	1.98 ± 0.07	178
G5	376 ± 6	1.43 ± 0.06	262	328 ± 3	1.32 ± 0.05	248	199 ± 4	1.94 ± 0.09	102
G6	320 ± 5	2.12 ± 0.05	151	282 ± 5	2.09 ± 0.09	135	210 ± 2	2.89 ± 0.08	73
G7	281 ± 8	2.79 ± 0.14	101	250 ± 1	3.16 ± 0.03	79	177 ± 2	4.63 ± 0.08	38
KJ	101 ± 1	4.20 ± 0.04	24	93.0 ± 2.2	5.30 ± 0.22	18	38.3 ± 1.0	5.45 ± 0.25	7.0
NR	217 ± 4	10.6 ± 0.3	20	168 ± 1	16.0 ± 0.1	11	169 ± 4	29.0 ± 1.6	5.8
IG2	162 ± 1	4.90 ± 0.05	33	105 ± 1	6.00 ± 0.12	18	53.8 ± 1.4	11.4 ± 0.6	4.7
PN	224 ± 2	2.05 ± 0.07	109	204 ± 1	2.05 ± 0.06	101	230 ± 5	6.99 ± 0.37	33

	N694F			N694W		
Substrate [b]	k_{cat} [c]	K_m [c]	k_{cat}/K_m	k_{cat}	K_m	k_{cat}/K_m
	s^{-1}	mM	s^{-1} mM^{-1}	s^{-1}	mM	s^{-1} mM^{-1}
G2	605 ± 8	2.11 ± 0.04	287	542 ± 2	1.34 ± 0.03	404
G3	646 ± 3	0.792 ± 0.014	816	312 ± 3	0.460 ± 0.004	678
G4	456 ± 9	1.04 ± 0.09	439	120 ± 1	0.375 ± 0.012	321
G5	461 ± 8	1.60 ± 0.04	289	154 ± 3	0.600 ± 0.015	257
G6	507 ± 5	2.92 ± 0.03	173	128 ± 3	1.29 ± 0.07	99
G7	472 ± 3	5.29 ± 0.04	89	112 ± 3	1.96 ± 0.06	57
KJ	80 ± 2.5	4.60 ± 0.04	18	37.6 ± 0.2	4.62 ± 0.04	8.1
NR	327 ± 6	20.0 ± 0.3	16	196 ± 1	24.5 ± 0.2	8.0
IG2	55 ± 1.4	2.60 ± 0.14	21	82.4 ± 0.4	2.27 ± 0.07	36
PN	150 ± 2	5.13 ± 0.14	29	164 ± 1	3.28 ± 0.06	50

[a]The parameters for G2 to G7 are from Tagami et al. (2013a).

[b]G2–G7, maltooligosaccharides with two to seven degrees of polymerization, respectively; KJ, kojibiose; NR, nigerose; IG2, isomaltose; PN, panose.

[c]All experiments were repeated three times and the values are represented as means ± SD.

Table 3 Initial transglucosylation velocities of wild-type and mutated ANGs in the presence of 100 mM G2

	v_{glc}	v_{PN}	v_{G3}	v_{CT}	v_h	v_{tg}	$R_{(1,4)}$[a]	$R_{(1,6)}$[b]	R_{tg}[c]
Enzyme	s^{-1} M^{-1}						%		
Wild type	980	314	101	24.3	270	439	23	72	62
N694A	943	323	94.9	13.2	256	431	22	75	63
N694L	1370	350	203	N.D.[d]	409	553	37	63	58
N694F	1410	305	377	25.5	351	708	53	43	67
N694W	916	278	193	N.D.[d]	223	471	41	59	68

[a]$R_{(1,4)}$, proportion of α-(1→4)-transfer vs. the total transglucosylation; [b]$R_{(1,6)}$, proportion of α-(1→6)-transfer vs. the total transglucosylation; [c]R_{tg}, proportion of transglucosylation in the total reaction. [d]The v_{CT} values for N694F and N694W were too low to be determined (N.D.).

Figure legends

Fig. 1. *Aspergillus niger* α-glucosidase (ANG)-catalyzed transglucosylation to form (A) panose (PN), (B) maltotriose (G3), (C) isomaltose (IG2), and (D) isomaltotriose (IG3). Circle, glucose unit; circle with slash, reducing-end glucose unit; transverse line between two circles, α-(1→4)-glucosidic linkage; wedge (^) between two circles, α-(1→6)-glucosidic linkage. The −1, +1 and +2 subsites are indicated as −1, +1, and +2, respectively. The left panels in A–D depict glucosyl-enzyme intermediates.

Fig. 2. Comparison of model structure of ANG (cyan) with sugar beet α-glucosidase (SBG; upper; PDB ID, 3weo; green) and the C-terminal subunit of maltase-glucoamylase (CtMGAM; lower; PDB ID, 3TOP; orange) (A) and multiple sequence alignment of the β→α loop 7 of the catalytic $(\beta/\alpha)_8$ barrel of GH31 α-glucosidases (B). (A) The residues associated with the formation of +1/+2 subsites are depicted by sticks. Numbers in parentheses indicate the residue number in SBG and CtMGAM, respectively. (B) Characters on the left side represent PDB IDs or UniProtKB accession numbers.

Fig. 3. Time courses of the products in the reaction of 100 mM G2 with (A) wild-type, (B) N694A, (C) N694L, (D) N694F, and (E) N694W ANG. ▲, glucose; △, G2; ○, PN; ●, IG2; ◆, G3; ◇, IG3, □, CT; ×, KJ; A1–E1, transglucosylation products; A2–E2, glucose and G2; A3−E3, magnified figures of A1–E1.

Fig. 4. Percentage composition of the transglucosylation products during a 3-h reaction. WT, wild-type ANG; A, N694A; L, N694L; F, N694F; W, N694W.

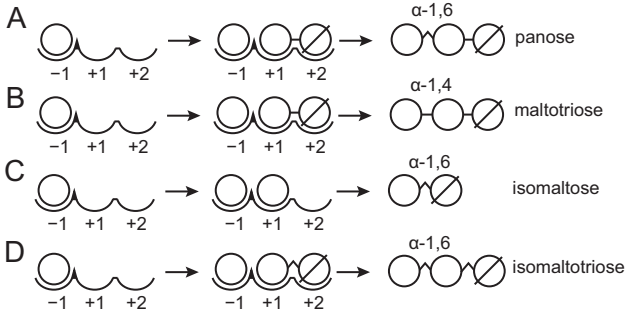

Fig. 1 (Min Ma, et al.)

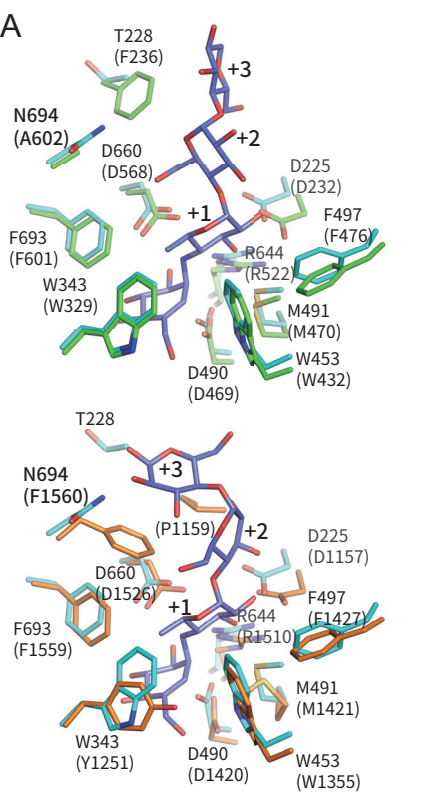

B

β7

UniProt or PDB	Organism/abbreviation										
PDBID_2g3m	*S. solfataricus*/MalA	V	G	C	D	I	G	G	F	Q	G	449
PDBID_5djw	*B. thetaiotaomicron*/BT_3299	S	G	A	D	I	G	G	F	L	F	375
Q9F234	*B. thermoamyloliquefacience*/BthGII	C	G	P	D	V	G	G	F	A	H	519
A0A0B6VK42	*B. sp*/BspAG31A	V	G	P	D	V	G	G	F	A	H	518
C1KIT5	*L. johnsonii*/LjAG31	A	G	T	D	I	G	G	F	G	A	510
PDBID_5dkx	*C. thermophilum*/GII	A	G	A	D	V	G	G	F	F	G	619
Q9US55	*S. pombe*/GII	S	G	A	D	V	A	G	F	F	G	635
PDBID_5f0e	*M. musculus*/GII;GANAB	C	G	A	D	V	G	G	F	F	K	566
PDBID_3n04	*B. obeum*/Ro-α-g	T	G	A	D	L	G	G	F	G	D	456
PDBID_3w37	*B. vulgaris*/SBG	I	G	A	D	I	C	G	F	A	E	546
D1MDV2	*H. vulgare*/Agl1;Agl97	I	G	A	D	I	C	G	F	N	G	569
PDBID_3top	*H. sapiens*/CtMGAM	T	G	A	D	I	C	G	F	F	Q	1562
P14410	*H. sapiens*/CtSI	T	G	A	D	I	C	G	F	F	N	1535
PDBID_2qmj	*H. sapiens*/NtMGAM	V	G	P	D	I	C	G	F	A	L	571
PDBID_3lpp	*H. sapiens*/NtSI	V	G	A	D	I	C	G	F	V	A	579
P10253	*H. sapiens*/GAA	V	G	A	D	V	C	G	F	L	G	651
A0PCH8	*A. niger*/ANG	F	G	A	D	T	C	G	F	N	G	695
Q12558	*A. oryzae*/AgdA	F	G	V	D	T	C	G	F	N	G	695
Q401B1	*S. occidentalis*/SOG	F	G	A	D	V	C	G	F	N	G	675
Q9C0Y4	*S. pombe*/SPG	V	G	A	D	V	C	G	F	L	G	682
Q75QW0	*A. implicatum*/Aig	V	G	S	D	V	C	G	F	G	G	656
B2B450	*P. anserina*/PAG	V	G	A	D	V	C	G	F	A	G	648
Q9C1S7	*A. nidulans*/AgdB	V	G	P	D	V	C	G	F	G	G	680
PDBID_4b9z	*C. japonicus*/CjAgdB31B	I	H	S	D	L	G	G	F	A	D	478
PDBID_5f7c	*B. thetaiotaomicron*/BT_0339	W	S	H	D	V	P	G	F	H	T	460

Fig. 2 (Min Ma, et al.)

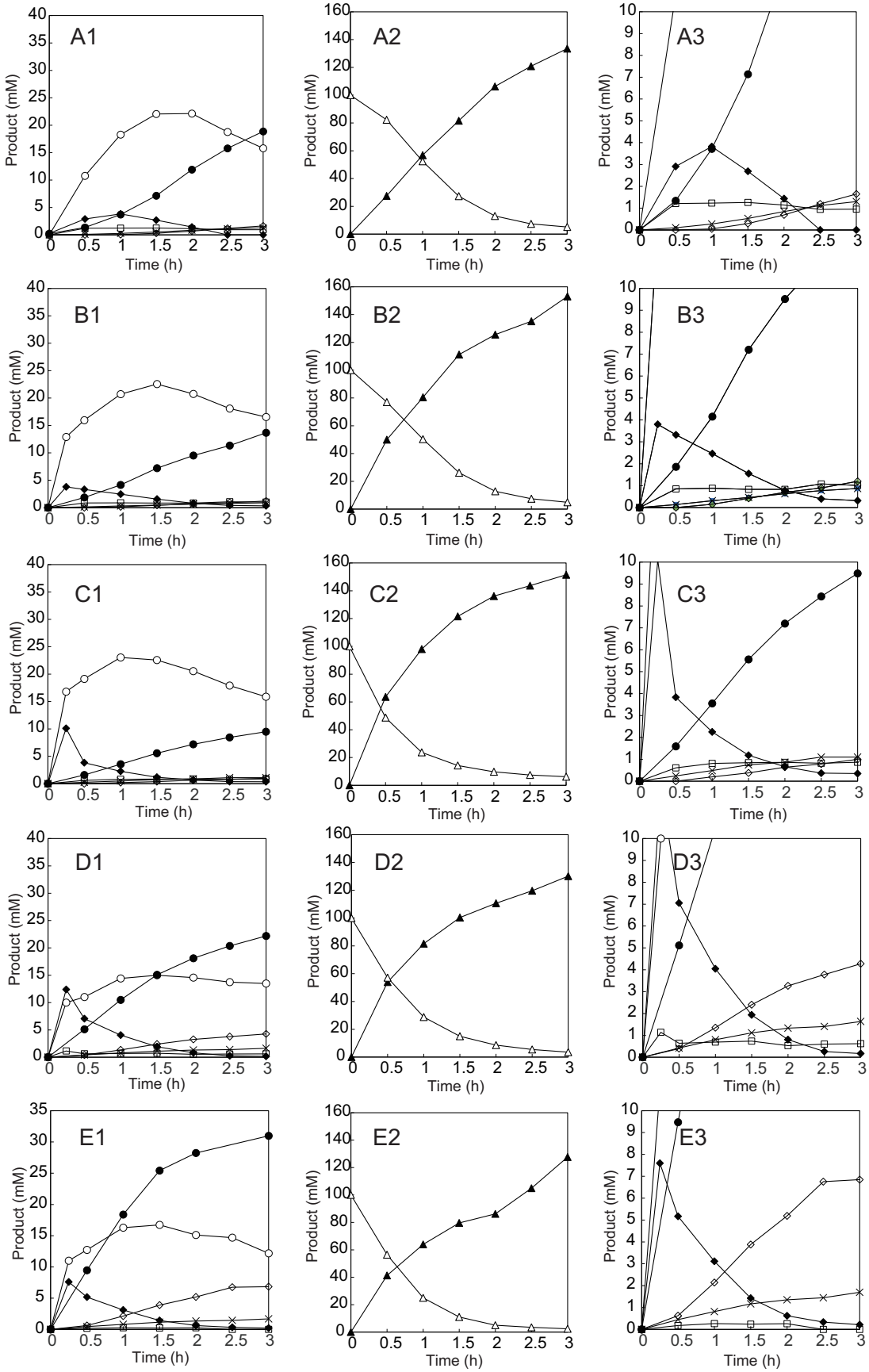

Fig. 3 (Min Ma, et al.)

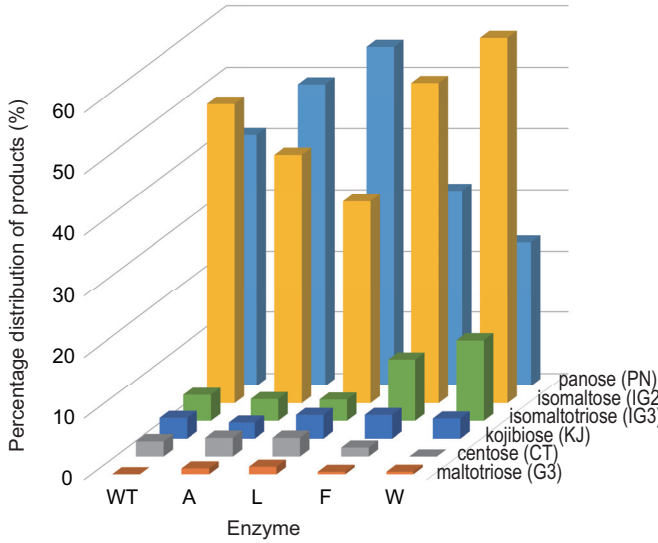

Fig. 4 (Min Ma, et al.)